

the cation exchange implies almost no change in the range of the O–C(H<sub>3</sub>) and V–O vibrations. For the potassium salt K<sub>8</sub>[V<sub>24</sub>O<sub>24</sub>(C<sub>4</sub>O<sub>4</sub>)<sub>12</sub>(OCH<sub>3</sub>)<sub>32</sub>] (**3**), the cubic structure of the anion, analogous to that of **2**, was determined by difference-Fourier analysis, whereas the potassium cations coordinated by methanol molecules as well as free solvent molecules in the crystal lattice were disordered and could not be clearly localized by crystal-structure analysis.<sup>[11]</sup> Exchanging the cations led to a change in the environment of the anion, which led to significant differences in the cation–anion interactions. Because of the ion-pair formation with tetra-*n*-butylammonium, a low charge formed, which is more likely a hydrophobic anion to be protected by the *n*-butyl groups. In the case of the potassium cation, the anion is highly charged, and balanced by the solvated potassium cations. This inevitably leads to compounds with different solubility behavior. Furthermore, the composition of the vanadium–oxygen compounds obtained by thermal decomposition can be controlled by the choice of cation. It is also advantageous that the squarato and methoxy ligands can be removed easily with a simultaneous reduction of the vanadium.

### Experimental Section

A 0.2 M solution of VO(OtBu)<sub>3</sub> (23 mL, 4.6 mmol) in methanol (Merck p.a.), H<sub>2</sub>C<sub>4</sub>O<sub>4</sub> (0.27 g, 2.4 mmol) and a 0.8 M solution of tetra-*n*-butylammonium hydroxide (2 mL, 1.6 mmol) in methanol (Fluka) were heated for 24 h at 125 °C in a 50 mL Teflon-lined autoclave (Berghof). After the autoclave was cooled to room temperature, the content was left to stand for one day at –30 °C to complete crystallization. The extremely temperature-sensitive, green crystals of **2** · *x* MeOH were filtered in an argon atmosphere at room temperature, washed with methanol, and dried under vacuum for a complete removal of the weakly bound methanol. Yield (based on the solvent-free compound): 0.71 g (0.12 mmol), 63%. Elemental analysis calcd (% based on the solvent-free compound) for C<sub>208</sub>H<sub>384</sub>N<sub>8</sub>O<sub>104</sub>V<sub>24</sub> (*M* = 5883.90 g mol<sup>–1</sup>): C 42.5, H 6.58, N 1.90; found: C 42.8, H 6.64, N 1.97; IR (KBr, 400–1600 cm<sup>–1</sup>):  $\tilde{\nu}$  = 424 (s), 464 (m) 573 (m), 967 (s), 976 (s) 1033 (s), 1069 (m), 1098 (w), 1446 (s), 1471 (s), 1523 cm<sup>–1</sup> (vs, br).

**3**: The synthesis of the potassium salt was analogous to that of the compound **2**, with a stoichiometric amount of potassium hydroxide instead of tetra-*n*-butylammonium hydroxide. Green crystals were isolated by filtering immediately after cooling the autoclave to room temperature. Yield (based on the solvent free compound): 0.36 g (0.084 mmol), 41%. Elemental analysis calcd (% based on the solvent free compound) for K<sub>8</sub>C<sub>80</sub>H<sub>96</sub>O<sub>104</sub>V<sub>24</sub> (*M* = 4256.9 g mol<sup>–1</sup>): C 22.6, H 2.27; found: C 21.5, H 2.32; IR (KBr, 400–1600 cm<sup>–1</sup>):  $\tilde{\nu}$  = 427 (s), 471 (m) 576 (m), 959 (s, br), 1013 (s, br), 1058 (m), 1099 (w), 1443 (s), 1483 (vs), 1521 cm<sup>–1</sup> (vs, br).

Received: April 24, 2001

Revised: July 25, 2001 [Z16992]

- [1] P. Gouzerh, A. Proust, *Chem. Rev.* **1998**, 98, 77–111.
- [2] a) D. E. Katsoulis, *Chem. Rev.* **1998**, 98, 359–388; b) J. Spandl, I. Brüdgam, R. Friese, H. Hartl, *Z. Kristallogr. Suppl.* **2000**, 17, 136.
- [3] M. I. Khan, J. Zubietta, *Prog. Inorg. Chem.* **1995**, 43, 1–149.
- [4] A. Müller, R. Rohlfing, E. Krickemeyer, H. Bögge, *Angew. Chem.* **1993**, 104, 916–918; *Angew. Chem. Int. Ed. Engl.* **1993**, 32, 909–912.
- [5] M. J. Khan, Y.-D. Chang, Q. Chen, J. Salta, Y. S. Lee, C. J. O'Connor, J. Zubietta, *Inorg. Chem.* **1994**, 33, 6340–6350.
- [6] M. Hilbers, M. Meiwald, R. Mattes, *Z. Naturforsch. B* **1996**, 51, 57–67.
- [7] K.-J. Lin, K.-H. Lii, *Angew. Chem.* **1997**, 109, 2166–2167; *Angew. Chem. Int. Ed. Engl.* **1997**, 36, 2076–2077.
- [8] J. Spandl, I. Brüdgam, H. Hartl, *Z. Anorg. Allg. Chem.* **2000**, 626, 2125–2132.
- [9] W. Prandtl, L. Hess, *Z. Anorg. Allg. Chem.* **1913**, 82, 103–129.
- [10] Crystal structure analysis of **2**: Bruker XPS diffractometer (CCD area detector, MoK $\alpha$  radiation,  $\lambda$  = 0.71073 Å), graphite monochromator,

empirical absorption correction using symmetry-equivalent reflections (SADABS, Area-Detector-Absorption Correction, Siemens Industrial Automation Inc., Madison, WI, **1996**); the structures were solved by direct methods; the initial structures were refined against *F*<sup>2</sup> (Bruker-SHELXTL, version 5.1, **1998**). The hydrogen atoms were calculated in geometrically idealized positions. Crystal size 0.40 × 0.38 × 0.24 mm, *T* = 133 K, triclinic, space group *P*1̄, *a* = 20.277(2), *b* = 20.605(2), *c* = 20.631(2) Å,  $\alpha$  = 115.07(1),  $\beta$  = 94.39(1),  $\gamma$  = 91.88(1)°, *V* = 7764.0(15) Å<sup>3</sup>, *Z* = 2,  $\rho_{\text{calcd}}$  = 1.258 g cm<sup>–3</sup>,  $2\theta_{\text{max}}$  = 47°, 54859 collected reflections, 22361 unique reflections, 1042 parameters,  $\mu$  = 0.76 mm<sup>–1</sup>, absorption correction, effective transmission max./min. = 0.7456/0.3775. *R*<sub>1</sub> (*I* > 2 $\sigma$ (*I*)) = 0.0718, *wR*<sub>2</sub> (*I* > 2 $\sigma$ (*I*)) = 0.1964, *R*<sub>1</sub> (all data) = 0.1149, *wR*<sub>2</sub> (all data) = 0.2166, largest difference peak and hole +/– = 1.767/0.743 e Å<sup>–3</sup>. The crystals were picked directly out of the mother liquor under a cold nitrogen stream. Because of the loss of the enclosed solvent methanol even at low temperatures, it was not possible to determine the number and exact positions of the remaining methanol molecules. Therefore, a solvent-free data set was generated with the computer program SQUEEZE (T. Spek, PLATON, **1999**). This data set was used for the crystal structure refinement.<sup>[12]</sup>

- [11] Crystal structure analysis of **3** (carried out analogously to details in reference [10]): tetragonal, *P*4/*ncc*, *a* = 26.356(3), *b* = 26.356(3), *c* = 31.290(5) Å, *V* = 21731.6 Å<sup>3</sup>, *T* = 143 K.<sup>[12]</sup>

- [12] Crystallographic data (excluding structure factors) for the structures reported in this paper have been deposited with the Cambridge Crystallographic Data Centre as supplementary publication nos. CCDC-162386 (**2**) and CCDC-169184 (anion substructure of **3**). Copies of the data can be obtained free of charge on application to CCDC, 12 Union Road, Cambridge CB2 1EZ, UK (fax: (+44) 1223-336-033; e-mail: deposit@ccdc.cam.ac.uk).

## 1,6-Methano[10]annulene has a Delocalized Structure in S<sub>0</sub> and S<sub>1</sub>: High-Resolution Spectroscopy in a Supersonic Jet\*\*

Reinhold Seiler and Bernhard Dick\*

Aromatic molecules substantially differ from olefins in terms of their reactivity and spectroscopic properties. A common characteristic and necessary structural element of aromatic molecules is a planar, cyclically conjugated system of 4*n* + 2  $\pi$  electrons, without bond-length alternation. The Hückel rule predicts that such systems are more stable than theoretical systems with alternating bond lengths.<sup>[1]</sup> This rule emerges from a molecular orbital (MO) description of the wavefunction of the  $\pi$  electrons, and has been verified by ab initio calculations for benzene and a number of other polycyclic arenes. For some species, however, calculations on the electron-delocalized structure found it to be a transition state between two electron-localized structures. A noted example of this effect is 1,6-methano[10]annulene (MA): The semiempirical MNDO, AM1, and PM3 methods obtained a localized structure while ab initio calculations at the SCF level with a simple STO-3G basis set favored delocalized

[\*] Prof. Dr. B. Dick, Dipl.-Chem. R. Seiler  
Institut für Physikalische und Theoretische Chemie  
Universität Regensburg  
93040 Regensburg (Germany)  
Fax: (+49) 941-943-4488  
E-mail: Bernhard.Dick@chemie.uni-regensburg.de

[\*\*] This work was supported by the Fonds der Chemischen Industrie.

electrons, yet the use of more extensive basis sets predicts that a localized structure is more stable.<sup>[2]</sup> Calculations accounting for correlation effects (CI or density functional theory (DFT)) again found that the delocalized structure is more stable, but the energy difference is only slight.<sup>[2]</sup> Evidently, the question of which state is really the lowest depends on the subtle interplay of various factors.

This behavior can be clarified with valence bond theory (VB) if the wavefunction  $\Psi$  of an annulene is represented as the weighted superposition of two basis states  $\psi_1$  and  $\psi_2$  with localized electron pairs and alternating bonds [Eq. (1)].

$$\Psi = c_1\psi_1 + c_2\psi_2 \quad (1)$$

Here, both  $\psi_1$  and  $\psi_2$  are exchanged in all formal single and double bonds in the ring perimeter. In the case of benzene, this represents the two Kekule structures. However, a matching pair of mesomeric structures exists for other aromatic rings, as shown in Figure 1 for benzene and MA.

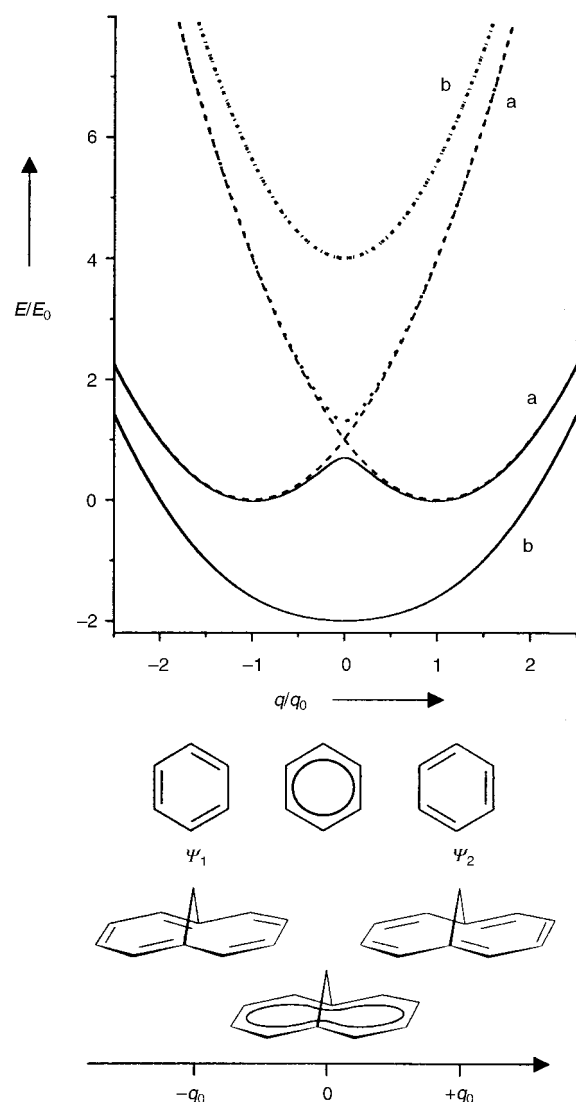


Figure 1. Potential function along the Kekule coordinate for an annulene with a) small and b) large resonance integral  $V$ . The curves of the uncoupled VB structures are dashed and those of the excited electronic states are dotted.

The coefficients of the wavefunction and their energy  $E$  are obtained from the Schrödinger equation [Eq. (2)], where  $H_1$  and  $H_2$  are the energy expectation values of the basis states and  $V$  is the resonance integral.

$$\begin{pmatrix} H_1 & V \\ V & H_2 \end{pmatrix} \begin{pmatrix} c_1 \\ c_2 \end{pmatrix} = E \begin{pmatrix} c_1 \\ c_2 \end{pmatrix} \quad (2)$$

These energy expectation values naturally depend on the electronic structure of the molecule;  $H_1$  minimizes at one Kekule structure,  $H_2$  at the other. Along the coordinate  $q$ , in which the transition between the two Kekule structures is represented, the energies increase quadratically with the harmonic approximation [Eq. (3) and (4)], where  $q_0$  and  $-q_0$  represent the electron-localized Kekule structures.

$$H_1 = E_0(q/q_0 + 1)^2 \quad (3)$$

$$H_2 = E_0(q/q_0 - 1)^2 \quad (4)$$

The two parabolas intersect at the point of the delocalized structure,  $q = 0$  (see the dashed curves in Figure 1). The nonvanishing resonance integral lifts the energetic degeneracy at  $q = 0$ . Two new potential functions thereby develop, which may be assigned to the electronic ground and excited state. The shape of the potential function for the ground state depends on the magnitude of the resonance integral. At  $V < E_0$  this potential has two minima for the localized structures, but only one minimum at the delocalized structure for  $V = E_0$ . Both cases are illustrated in Figure 1 as curves (a) and (b) (for each case the solid line represents the ground state and the dashed curve the excited state). It is thus conceivable that molecules, which formally obey the Hückel rule, actually have a localized ground state. A double-minimum potential is in fact found for some homoaromatic systems, such as semi-bullvalene.<sup>[3]</sup>

In arenes,  $V > 0$  because both VB wavefunctions have an uneven number of electron pairs.<sup>[4]</sup> The wavefunction  $\Psi_u$  of the excited state corresponds in this case to the antisymmetric linear combination, which, in the case of MA (space group  $C_{2v}$ ), belongs to the irreducible representation  $B_1$ . This state is in turn equivalent to the  $L_b$  state of MO theory. The electronic transition from the ground state is polarized along the long molecular axis. Of note, the VB model predicts that the excited electronic state should be always delocalized, and indeed with simple basis sets or semiempirical methods one finds that the first excited electronic state for MA is such a delocalized  $B_1$  state. If the ground state is likewise delocalized, then the VB model predicts that the vibrational frequency, which belongs to the normal coordinate  $q$  (the Kekule mode), should be low in the ground state but very high in the excited state.

Recently, the symmetry of the electronic ground state of MA was investigated by IR and Raman spectroscopic measurements.<sup>[5]</sup> Because of the good agreement of the measured frequencies and intensities with highly detailed ab initio calculations (DF/B3LYP, 6-31G\*\*), the ground state

of the delocalized structure was assigned  $C_{2v}$  symmetry. In this space group, all vibrations are Raman active but those in the  $a_2$  representation are IR inactive. However, no information on their polarization was gained to allow assignment of the vibrations to irreducible representations.

Herein we present measurements of the vibrational structure of the excited electronic state, which confirm the assumption of the delocalized structure of the ground state. If the ground state of MA had an energetic double minimum, then the electronic excitation would necessitate significant electronic structural changes. Following the Franck–Condon principle, the vertical transition should have the greatest intensity and the electronic origin of the absorption band should be only weak. In contrast, when both states have delocalized structures, one expects an intense electronic origin. Explicit evidence requires a spectrum of the excited state, in which the intensities and symmetries of the individual vibrational transitions can be determined. The first electronic transition of MA is, however, intrinsically very weak, a consequence of the pseudoparity selection rule, which is also responsible for the low intensity of the first band of naphthalene.<sup>[6]</sup> Hence additional lines may appear in the spectrum which gain their intensity by Herzberg–Teller coupling with higher electronic states. That such vibrationally induced transitions contribute to the spectrum has been concluded already from the fact that the degree of polarization of the transition varies over the bands.<sup>[7]</sup> The low resolution of the spectra in solution and organic glasses at low temperatures prevents separation of the vibrational transitions from each other. Measurement of samples in Shpol'skii matrices at 15 K still shows broad zero-phonon lines and even broader phonon sidebands.<sup>[2]</sup>

Unambiguous, highly resolved spectra are available from isolated, ultracold MA in a supersonic jet. Such a fluorescence excitation spectrum of the  $S_0 \rightarrow S_1$  transition is shown in Figure 2. For these conditions the single vibronic lines show widths of about  $1\text{ cm}^{-1}$ , equivalent to a rotational temperature of 2 K. The most intense line is the longest wavelength transition assigned to the electronic origin. Double-resonance measurements show that some weak lines in Figure 2, marked

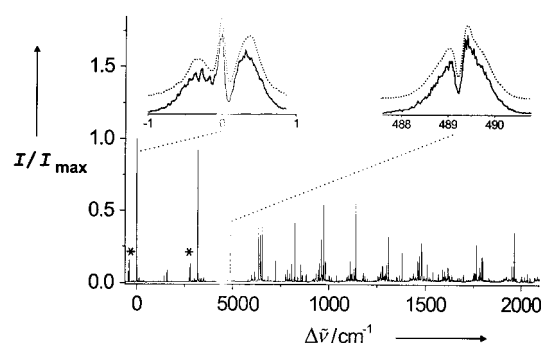


Figure 2. Fluorescence–excitation spectrum of the  $S_0 \rightarrow S_1$  transition of MA in a supersonic jet. The rotational envelope of the electronic origin at  $25154\text{ cm}^{-1}$  and the vibronic band at  $489\text{ cm}^{-1}$  above the origin is enlarged. A comparison with simulated band contours, represented as dotted lines above the experimental bands, unambiguously proves the transition moment which, for the electronic origin, lies along the long axis and for the vibronic band lies along the short axis of the perimeter.

with an asterisk, stem from another species, most probably a van der Waals dimer of MA formed during the jet expansion. The spectrum of MA shows many lines attributable to progressions and combinations of a few fundamental vibrations, these are given in Table 1. The vibrational frequencies

Table 1. Wavenumbers of the vibrations [ $\text{cm}^{-1}$ ] in the irreducible representations  $a_1$  and  $a_2$  for the excited electronic state.

Theory	$a_1$	Experiment	Theory <sup>[a]</sup>	$a_2$	Experiment <sup>[b]</sup>
186		159	161		143
354		318	387		350
506		477	539		489
700		643	782		725
720		655	940		856
869		824	967		947
929		884	1133		1142
998		975	1299		1301
1315		1310 <sup>[c]</sup>	1405		1379
1479		1479	1593		1590
1577		1568	1714		1698
1631		1617			
1680		1669			

[a] CAS ab initio calculation (6-31G basis).<sup>[2]</sup> [b] This work. [c] This line coincides with the  $\Delta n = 2$  transition of the mode at  $\nu = 655\text{ cm}^{-1}$ .

are in good agreement with the results of the best available ab initio calculations.<sup>[2]</sup> The highly resolved measurement gave the rotational structure for each band, two examples of which are shown in Figure 2. From the characteristic structure exhibited by these bands, the electronic origin at  $25154\text{ cm}^{-1}$  is shown to be polarized along the long axis of the perimeter. The electronic wavefunction of the excited state belongs therefore to the irreducible representation  $B_1$  of the  $C_{2v}$  point group. The excited wavefunction of the VB model described above also belongs to this representation. Likewise the first transition of naphthalene is polarized along the long molecular axis. Vibronic bands with this polarization correspond to totally symmetric vibrations (the irreducible representation  $a_1$ ). The vibronic band at  $489\text{ cm}^{-1}$  is polarized along the short axis and must be assigned to a vibration with  $a_2$  symmetry.

A quantitative analysis of the band shapes yields rotational constants for  $S_0$  and  $S_1$ . The very good agreement with the rotational constants for the ab initio (MP2/6-31G) calculated electronic structure of  $S_0$  is a further indication of a delocalized structure. From these rotational constants the band shapes for the vibronic transitions polarized vertical to the perimeter may be calculated. Bands with this shape, which belong to vibrations of  $b_1$  symmetry, were not observed. This result also supports the assumption of a delocalized structure. If MA had alternating bonds in the ground state, a progression in the Kekule mode with  $b_1$  symmetry must appear. Progressions in only two modes, at wavenumbers 318 and  $655\text{ cm}^{-1}$ , were observed. The rotational structure of these lines shows that both modes are totally symmetric. Hence the changes in geometry upon electronic excitation can largely be described with these two coordinates, whereby the molecular symmetry remains unchanged. In all progressions the intensity monotonously decreases with increasing energy. The

electronic origin is the most intense band of the complete spectrum. The structural changes are therefore smaller than the elongation of the classical harmonic oscillator at the zero-point energy, otherwise the intensity would initially increase with increasing quantum number. The electronic ground state also has the same symmetry and almost the identical geometry as the electronic excited state. For the latter, only the delocalized structure is applicable, and hence this structure must also be assigned to the ground state.

### Experimental Section

MA was synthesized following the method of Vogel and Roth<sup>[8]</sup> and purified by distillation. The ultracold supersonic jet was produced by the expansion of a mixture of MA (1.3 mbar) along with the helium carrier (2 bar) through a pulsed nozzle of 0.5 mm diameter. A dye laser pumped by an excimer laser was used for fluorescence excitation, and a second dye laser/excimer laser pair was used for the double-resonance measurements. The laser bandwidth (FWHM) limited resolution to 0.2 cm<sup>-1</sup> in the survey spectra; for the measurement of the rotational structures a Fabry–Perot interferometer inside the laser cavity improved the resolution to 0.1 cm<sup>-1</sup>.

Received: June 8, 2001 [Z17252]

- [1] E. Hückel *Z. Phys.* **1931**, 70, 204–286; P. J. Garratt, *Aromaticity*, Wiley, New York, NY, **1986**.
- [2] L. Catani, C. Gellini, P. R. Salvi, *J. Phys. Chem. A* **1998**, 102, 1945–1953.
- [3] R. V. Williams, *Eur. J. Org. Chem.* **2001**, 227–235.
- [4] S. Zilberg, Y. Haas, *Int. J. Quantum Chem.* **1999**, 71, 133; S. Zilberg, Y. Haas, *J. Phys. Chem. A* **1998**, 102, 10843–10850.
- [5] C. Gellini, P. R. Salvi, E. Vogel, *J. Phys. Chem. A* **2000**, 104, 3110–3116.
- [6] R. Pariser, *J. Chem. Phys.* **1956**, 24, 250–268.
- [7] H. J. Dewey, H. Deger, W. Frölich, B. Dick, K. A. Klingensmith, G. Hohlneicher, E. Vogel, J. Michl, *J. Am. Chem. Soc.* **1980**, 102, 6412–6417.
- [8] E. Vogel, H. D. Roth, *Angew. Chem.* **1964**, 76, 145; *Angew. Chem. Int. Ed. Engl.* **1964**, 3, 228–229; E. Vogel, W. Klug, A. Breuer, *Org. Synth. Coll.* **1987**, 6, 731–736.

## Silynes (RC≡SiR') and Disilynes (RSi≡SiR'): Why Are Less Bonds Worth Energetically More?\*

David Danovich, François Ogliaro, Miriam Karni,  
Yitzhak Apeloig,\* David L. Cooper,\* and Sason Shaik\*

*Dedicated to Professor Zvi Rappoport  
on the occasion of his 65th birthday*

Since the first isolation in 1981 of stable silaethylene<sup>[1]</sup> and disilene<sup>[2]</sup> a variety of new compounds containing doubly bonded silicon have been synthesized and their chemistry explored.<sup>[3]</sup> The next challenge has become the syntheses of compounds in which silicon has a triple bond.<sup>[4]</sup> Until recently HSi≡N was the only known silicon species with a triple bond, and was prepared by matrix isolation and identified by UV and infrared (IR) spectroscopy.<sup>[5a]</sup> Other attempts to isolate RSi≡N resulted in the isomeric RNSi species.<sup>[5b–g]</sup> While the formation of transients of the form RSi≡SiR (R = Me<sup>[6a]</sup> and Tip<sub>2</sub>C<sub>6</sub>H<sub>3</sub>,<sup>[6b]</sup> (Tip = 2,4,6-triisopropylphenyl)) was suggested, no conclusive evidence has been presented to support these assignments. Only recently has the existence of stable FSi≡CH and ClSi≡CH, under gas-phase conditions, been demonstrated.<sup>[7]</sup> This successful assignment followed previous theoretical predictions.<sup>[8]</sup> The computational studies<sup>[7–9]</sup> have shown, however, that HSi≡CH and HSi≡SiH possess a *trans*-bent geometry (Figure 1, **1B** and **2B**) in contrast to the linear geometry of acetylene (**3**). Moreover, the linear isomers **1L** and **2L** are not even minima on the potential-energy surface (substituted silynes and disilynes behave likewise<sup>[7, 8, 9d]</sup>). *Trans*-bending appears also in analogous E≡E species (E = Ga, Ge, Sn, Pb) which are formally triply bonded,<sup>[10]</sup> and it seems to be a characteristic feature of multiple bonding in higher-row compounds. The inherent preference for bending raises fundamental questions about the nature of CSi or SiSi bonding.<sup>[11]</sup> Is it truly a triple bond such as C≡C? What is the

- [\*] Prof. Y. Apeloig, Dr. M. Karni  
Department of Chemistry and  
The Lise Meitner-Minerva Center for Computational Quantum  
Chemistry  
Technion-Israel Institute of Technology, 32000 Haifa (Israel)  
Fax: (+972) 4-8294601  
E-mail: chrappel@technion.ac.il
- Dr. D. L. Cooper  
The Department of Chemistry  
University of Liverpool  
P.O. Box 147, Liverpool L69 7ZD (UK)  
Fax: (+44) 151-794-3588  
E-mail: dlc@liv.ac.uk
- Prof. S. Shaik, Dr. D. Danovich, Dr. F. Ogliaro  
The Department of Organic Chemistry and  
The Lise Meitner-Minerva Center for  
Computational Quantum Chemistry  
The Hebrew University, 91904 Jerusalem (Israel)  
Fax: (+972) 2-6584680  
E-mail: sason@yfaat.ch.huji.ac.il

[\*\*] The research is supported by an Israel Science Foundation (ISF) and a Niedersachsen grant (to S.S.), by a U.S.–Israel Binational Science Foundation (BSF) grant (to Y.A.) and by the Minerva Foundation. S.S. and F.O. thank the European Union for a Marie Curie Fellowship (Contract number: MCFI-1999-00145). S.S. and D.D. thank P. C. Hiberty for the helpful advice.